Supporting Information

Inaba and Kawano 10.1073/pnas.1401370111

SI Text

Spatial Tuning Curves of the Neuronal Responses. To characterize the neuron's spatial tuning profile for each of the behavioral conditions, we quantified the neuronal responses to the moving stimulus located at 20 locations. We fitted a Gaussian function involving four free parameters to the neuronal responses obtained from individual trials over a time period of 50–150 ms after stimulus onset and 50–150 ms after saccade onset (Fig. S2) as follows:

$$y(\theta) = B + A \cdot \exp\left\{-0.5 \cdot ((\theta - \theta_0)/\sigma)^2\right\}, \quad \textbf{[S1]}$$

where B, A, θ_0, and σ denote the baseline firing rate, maximal amplitude, optimal location, and tuning width, respectively (1). The parameter values of the best-fit function were used to quantify the spatial tuning profiles. We defined the stimulus location inside and outside the receptive field (RF) as within the range between $\theta_0 \pm \sigma^2$ and out of the range between $\theta_0 \pm 3\sigma^2$, respectively. We regarded a neuron as having significantly increased its firing rate if the mean response in the RF was larger than the mean plus 2SD of baseline activity out of the RF. As a robust test of statistical significance, we have used two-sided Wilcoxon rank sum tests between the mean responses inside and outside the RF.

Postresponse/Preresponse Ratio. To assess the influence of saccades on neuronal responses, we calculated a postresponse/preresponse ratio (defined as $[(R_{post}/R_{pre})] \times 100\%$), where R_{post} and R_{pre} are the mean firing rates after the saccade (50–150 ms after saccade onset) and before the saccade (50–150 ms after stimulus onset), respectively (Fig. S3). A small positive value (<100%) indicates that the response after the saccade is weaker than that after the stimulus onset. In paradigm I, when the moving grating was turned on in the RF (RF1) or brought into the RF by saccades (RF2), relatively similar responses were observed for neurons recorded in medial superior temporal (MST) area (n = 118, ratio = 89.7 ± 34.5%; median ± SD) and middle temporal (MT) area (n = 46, ratio = 90.7 ± 56.1%; median ± SD) (Fig. S3*A*, two-sided Wilcoxon rank-sum, $P > 0.05$). There were some neurons in both areas that had a small value of the postresponse/preresponse ratio (50% or less), as they showed very strong responses to the onset of the moving grating but not as large responses when the saccade brought the stimulus into their RF. However, on average in paradigm I, the neuronal population responded to the stimulus similarly (~90%) when the visual stimulus was turned on in the RF and when the saccade brought the stimulus into the RF.

In contrast, in paradigm II, when the moving grating was turned off before saccades, virtually no response was observed after saccade in MT neurons (n = 41, ratio = 10.2 ± 7.5%; median ± SD; Fig. S3*B*). However, most MST neurons discharged when a saccade brought the location of the visual stimulus into their RFs, where the visual stimulus itself was no longer presented at that time. The mean amplitude of the neuronal response to the visual memory trace was weaker than that to the real stimulus (n = 98, ratio = 53.4 ± 34.5%; median ± SD; Fig. S3*B*), significantly different from MT (two-sided Wilcoxon rank sum, $P < 0.01$). Similar effects of the saccades on the responses of MST (n = 42, ratio = 53.9 ± 26.1%; median ± SD) and MT (n = 12, ratio = 18.1 ± 5.6%; median ± SD) neurons were observed in paradigm III (Fig. S3*C*; two-sided Wilcoxon rank sum, $P < 0.01$).

Effect of Phosphor Persistence of the Cathode Ray Tube Display. In consideration of the effect of phosphor persistence of the cathode ray tube (CRT) display that might cause neuronal responses to the visual stimulus that had been turned off a while ago, we conducted additional experiments by using a mirror galvanometer system with a mechanical shutter (paradigms I-2 and II-2). The procedures used in the present study are similar to those previously described (2).

The animal was seated in a dark room and faced a translucent tangent screen subtending 80° × 80° at the viewing distance of 40 cm. A red spot (the fixation point or saccade target, 0.3° in diameter) and a grating pattern were backprojected onto the screen by a light-emitting diode projector and a slide projector, respectively. The sinusoidal grating pattern with spatial frequencies of 0.6 cyc/° were moved with mirror galvanometers in the light paths (Fig. 1*A*). To map the location of the RF, the moving grating pattern was presented in a narrow strip, which was horizontal (80° wide and 4° tall) or vertical (4° wide and 80° tall) as dividing the size of screen into 20 strips (either horizontal or vertical). An electromechanical shutter in the light path was used to turn the grating stimulus on and off (opening and closing time, <5 ms). The task sequence was the same between paradigm I and paradigm I-2 (Fig. 1*A*). Between paradigm II and paradigm II-2, only the timing of the stimulus offset was different from each other. In paradigm II-2, disappearing the stimulus was triggered by saccade onset (Fig. 2*A*). During the experiment, the saccade onset was defined as the time when the monkey broke the fixation and his eyes moved out from the 1.5° × 1.5° window.

We recorded 23 neurons in MST during paradigms I-2 and II-2. All of the neurons increased their activities after saccades, even when the visual stimulus had already gone [*SI Text*, *Spatial Tuning Curves of the Neuronal Responses*]. In paradigm I-2, the neuronal population responded to the stimulus similarly when the visual stimulus was turned on in the RF1 and when the saccade brought the stimulus into the RF2 (postresponse/preresponse ratio = 85.9 ± 39.8%; median ± SD; Fig. S4*A*). When the moving grating was turned off before saccades in paradigm II-2, most MST neurons still discharged when a saccade brought the location of the visual stimulus into their RFs (postresponse/preresponse ratio = 70.8 ± 32.2%; median ± SD; Fig. S4*B*). There was no significant difference between the results obtained by the CRT display (Fig. S3 *A* and *B*) and the mirror galvanometers (Fig. S4 *A* and *B*) (two-sided Wilcoxon rank sum, $P > 0.05$).

To compare with the results from the CRT display and the mirror galvanometer system, we applied the sliding-window receiver operating characteristic (ROC) analysis to the data obtained from individual trials throughout the period of saccades during paradigm II-2 (*Materials and Methods*). Fig. S4*C* illustrates the time course of the area under the ROC curve (AUC) as a classifier for the stimulus in RF1 and RF2. For MST neurons (n = 23), the AUC for RF1 increased after the stimulus onset and remained high before the saccade and then waned after the saccade, and the AUC for RF2 significantly increased after the saccade offset. The median AUC from 50 to 100 ms after the saccade offset was 0.88 ± 0.29 (Fig. S4*D*). Thus, no significant difference was observed between the results obtained by the CRT display (Fig. 5*B*) and the mirror galvanometers (Fig. S4*D*) (two-sided Wilcoxon rank sum, $P > 0.05$). Therefore, the results support the assumption that the responses after the saccade were evoked by the memory of the preexisted stimuli, but not by the persisted phosphor of the CRT display.

1. Funahashi S, Bruce CJ, Goldman-Rakic PS (1990) Visuospatial coding in primate prefrontal neurons revealed by oculomotor paradigms. *J Neurophysiol* 63(4): 814–831.

2. Inaba N, Shinomoto S, Yamane S, Takemura A, Kawano K (2007) MST neurons code for visual motion in space independent of pursuit eye movements. *J Neurophysiol* 97(5): 3473–3483.

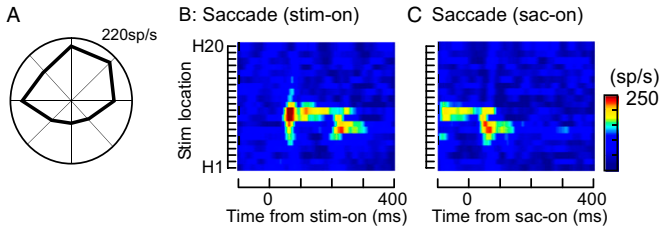

Fig. S1. (*A*) Polar plot of the direction tuning of the MST neuron shown in Figs. 1–3 defined by a moving random-dot pattern in eight directions during fixation. (*B* and *C*) Spatiotemporal RF map of the MST neuron during leftward 10° saccade. Responses are aligned at stimulus onset (*B*) or saccade onset (*C*).

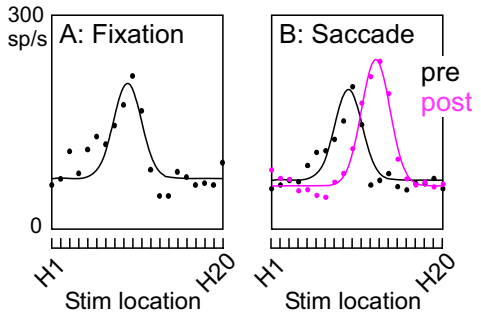

Fig. S2. (*A*) Spatial tuning curves of the neuronal responses of the MST neuron to the moving stimulus located at 20 horizontal locations in the fixation task. Each point shows the mean firing rate over a period from 50 to 150 ms after the stimulus onset. (*B*) Spatial tuning curves of the MST neuron in the saccade task of paradigm I. Each point shows the mean firing rate over a period from 50 to 150 ms after the stimulus onset (black) and 50–150 ms after the saccade onset (magenta), respectively.

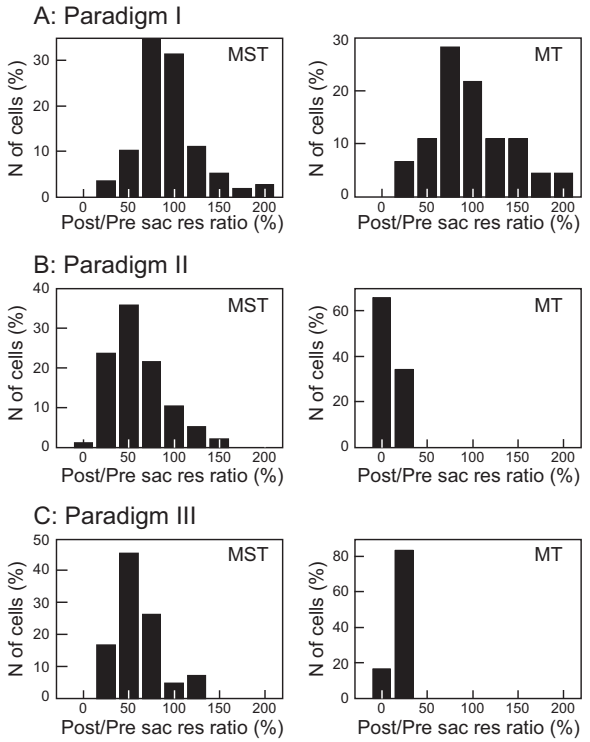

Fig. S3. Comparison of postresponse/preresponse ratio between MST and MT neurons. (*A–C*) Distribution of the postresponse/preresponse ratio of MST (*Left*) and MT (*Right*) neurons. (*A*) Paradigm I, (*B*) paradigm II, and (*C*) paradigm III.

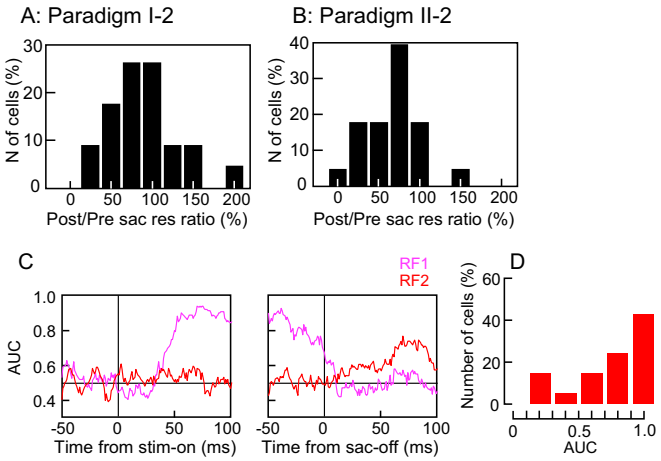

Fig. S4. (*A* and *B*) Distribution of the postresponse/preresponse ratio of the 23 MST neurons. (*A*) Paradigm I-2 and (*B*) paradigm II-2. (*C*) The time course of the AUC as a classifier for the stimulus in RF1 (magenta) and RF2 (red). For MST neurons, the AUC for RF2 significantly increased after the saccade. (*D*) Distribution of the mean AUC from 50 to 100 ms after the saccade offset for the MST neurons.